Expanding the Versatility of a More Accurate Accelerated Monte Carlo Simulation for 3D PET: Data Correction of PET Emission Scans Using ^{124}I

C.H. Holdsworth, M. Dahlbom, A. Liu*, L. Williams*, C. S. Levin**, M. Janecek

E.J. Hoffman

UCLA School of Medicine, City of Hope*, UCSD School of Medicine** and San Diego VA Medical Center**

Abstract--**Our Monte Carlo PET simulation for a 3D PET scan is able to simulate ~5 million coincidence events per minute per minute on 300MHz Sun dual processor workstation. This is over two orders of magnitude faster than most other available Monte Carlo simulations for 3D PET and is fast enough to be employed as a scatter correction for 3D PET imaging. We have improved the accuracy of our simulation of a clinical ECAT HR+ scanner by analyzing the effect of the energy response of the detectors on simulated sinograms.**

We created a modified version of our simulation for 3D PET scans using ^{124}I. Our initial version was five times slower than our simulation for FDG scans. We analyzed the distribution of the simulated detected coincidence events involving gamma rays and proposed an analytical method that corrected for these events. We found that this correction is subject to errors that can be exacerbated when used in conjunction with an analytical scatter correction that scales to the measured sinogram's scatter tail. To reduce error, we have developed a faster, more detailed simulation for ^{124}I. We are currently investigating the possibly of a fully Monte Carlo correction for both scatter and gamma ray coincidences in the future.

I. Introduction

Due to the ~20% energy resolution of BGO crystals, there is not a sharp cutoff in the energy discrimination of clinical scanners such as the ECAT HR+. Because the energy threshold can be set as low as 350keV, photons striking a detector have an energy-dependant probability of being detected [1]. The true energy response for a particular scanner is difficult to measure to a high degree of accuracy.

The actual energy response of detectors has a direct effect on the distribution of scatter in raw scan data. We ran simulations and compared simulated sinograms with the measured sinogram. By adjusting the simulated energy response, we determined the energy response distribution to use in our simulation that resulted in the most accurate results. This optimal simulated energy response will be similar to the true energy response of the scanner, though it would not contain effects not considered in the simulation.

The injection of radioactive labeled antibodies for radioimmunotherapy is becoming more important in the treatment of various cancer types. An important aspect in radioimmunotherapy is the accurate determination of the distribution of a tracer that mimics the behavior of the administered radiation dose. This typically involves either planar or SPECT imaging. These methods have inherent shortcomings that limit the accuracy of the dose estimates. In planar imaging, one cannot separate the overlying tissues or accurately correct for attenuation. Although there are significant improvements in scatter and attenuation correction techniques in SPECT, the quantitative accuracy is limited. On the other hand, PET has been shown in numerous research studies to have high quantitative accuracy; however, PET imaging is typically limited to relatively short-lived isotopes that are not suitable for imaging the uptake of antibodies [2].

Single photon emitting isotopes of iodine are the most commonly used labels for antibodies for in-vivo imaging in humans. In addition to the limited quantitative accuracy of single-photon imaging, these isotopes have additional limitations such as to long or short half-life (^{123}I 13 hrs, ^{125}I 60 days) or energies are sub-optimal for imaging (^{123}I 35 keV, ^{131}I 364 keV). ^{124}I, a positron emitter with a half-life of 4.2 days, could potentially be used as a substitute for these single photon emitters. This isotope also has some limitations, such as a low yield of positrons, relatively high positron energy, and coincident emission of multiple gamma rays [2]. Approximately half of the detected coincidences (after subtraction of the delayed events) are caused by detection of concidences involving these gamma rays.

Our Monte Carlo PET simulation for 3D PET scans is ~200 times faster than most other available Monte Carlo simulations for 3D PET [3,4]. We have developed versions of our simulation that simulate 3D PET scans using ^{124}I. We have used the simulation to analyze the form of coincidence events that involve a gamma ray and are investigating analytical and Monte Carlo corrections for these events.

0-7803-7324-3/02/$17.00 © 2002 IEEE

II. Materials and Methods

A. Phantoms, 3D PET Scanners, and Input Images

To obtain our original measured sinogram data for the ^{124}I study, we used a Jaszczak phantom. The phantoms were scanned using a Siemens/CTI 962 HR+ PET scanner with septa removed. 2D transmission scan data was processed to generate the transmission image and 3D attenuation correction data. For simulation accuracy studies, we used data from four-hour transmission scans to reduce noise and increase accuracy in the transmission image. This image contains the attenuation coefficient of the simulated subject.

We also acquired four-hour emission scans to reduce noise in the emission image. The image intensity in each voxel of this emission image is used to determine the number of annihilations simulated in that voxel. We used the scanner's simulation-based scatter correction [5] during image reconstruction to provide a more accurate initial activity distribution estimate for the simulation. We have seen that noise and error in the input images can result in significant error in simulation sinograms and images.

B. Our Monte Carlo Simulation

Most Monte Carlo simulations for 3D PET [6,7,8,9] would take on the order of a day to simulate the equivalent of 20 million scatter coincidence events on a 300MHz dual processor [10,11]. Our Monte Carlo PET simulation for 3D PET is able to generate 20 million scatter coincidence events in 8 minutes [3]. Our simulation is accurate and is fast enough to be employed as a scatter correction for 3D PET imaging. We have developed versions of our simulation that simulate 3D PET scans using ^{124}I that incorporates coincidence emissions involving gamma rays.

C. Initial 124I Simulation for ECAT HR+ Scanner

Our initial simulation for ^{124}I only took into account positron emissions and positron emissions in coincidence with a 602KeV photon. This was five times slower than the FDG simulation, so we used simulation results to develop a fast, clinically feasible analytical correction for gamma ray events. We recently developed a new, faster version that takes into account all possible coincidence emissions.

D. Current ^{124}I Monte Carlo Simulation

Our current ^{124}I simulation incorporates over 99% of all possible coincidences that can result when I^{124} decays. This faster code is much more complex than the initial version and simulates 31 different possible coincidence emissions.

The following are variance reduction techniques we have implemented in our new simulation. When the first (or one of the first two for triplet emissions) photon of a coincidence emission is detected, multiple second (or last) photons are simulated. Also, when the first two photons out of three emitted gamma rays are detected, the third isn't simulated. Instead, the coincidence event is given an appropriate weight.

In addition, currently all high energy photons that hit the gantry are detected. This means that simulation sinograms must be scaled to the measured sinogram. For better accuracy, we plan to take into account the detector energy response without sacrificing efficiency by adjusting the number of simulated high-energy photons such that the simulation weight of each is close to 1. Currently photons emissions are allowed in any direction. We plan to restrict the initial direction of emitted photons to increase simulation efficiency without compromising accuracy. We expect significant increases in the current efficiency as more variance techniques are implemented.

III. Results

A. Scatter Distributions and Detector Energy Response

We ran a simulation of a cylindrical phantom and stored coincidence events involving scattered photons of different energy ranges into different simulated sinograms. This gave us the opportunity to observe the effect of scattered photon energy on resulting sinograms, see figure 1.

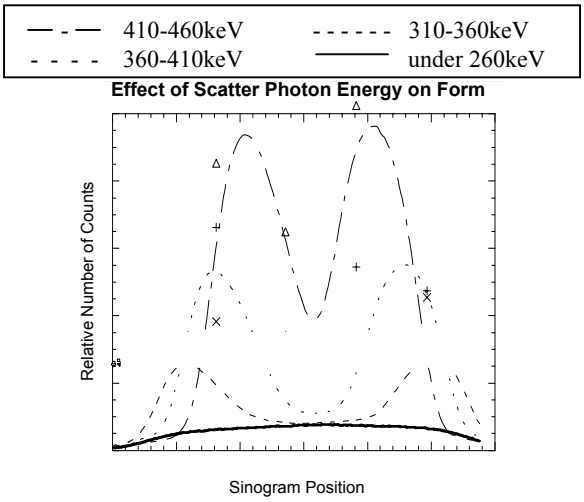

Figure 1. Distributions of coincidence events that include only scattered photons in specific energy range. Scattered photons of a given energy result in a characteristic peak at a specific sinogram location (for scattered photon energies > ~260KeV).

Because scatter angle depends on the energy of the scattered photon, a singlely scattered photon in coincidence with a primary photon will contribute to a specific peak position in the sinogram characteristic of that energy. As a result, scattered coincidence event distributions for different energies have distinct shapes when above 260KeV.

The specific location of differences between simulation sinograms and measured sinograms may indicate an error in the simulated detector response for a specific energy. By adjusting the simulated detector energy response so that sinograms match everywhere, you can get a measure of the actual energy response. Figure 2 shows the energy response that resulted in the most accurate simulation sinogram. Differences between this and measured energy response [1] can be due experimental errors such as multiple scatter or

interference from primary photons or due to simulation errors such as depth of interaction, block effects, variability in BGO penetration length, or input image error.

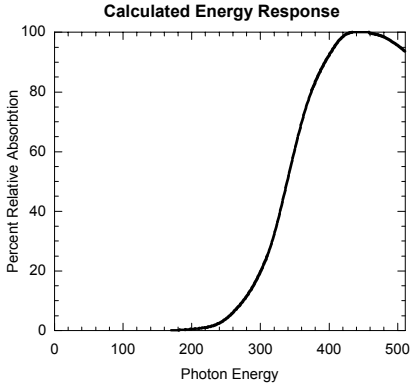

Figure 2. Graph of the simulated energy response that resulted in the most accurate simulated results. It is an approximation of true energy response.

The most significant difference in the simulated energy response was that scattered photons with energies near 450keV were observed to have greater detection efficiency than higher energy annihilation photons. We believe this is a real effect that could not be observed in the experimental measure due to the overlap of primary photons, affected by non-colinearity and source thickness, with high energy scattered photons. The drop in detection efficiency near 511keV may be due to photons that deposit only a small amount of energy in detectors before escaping, see figure 3.

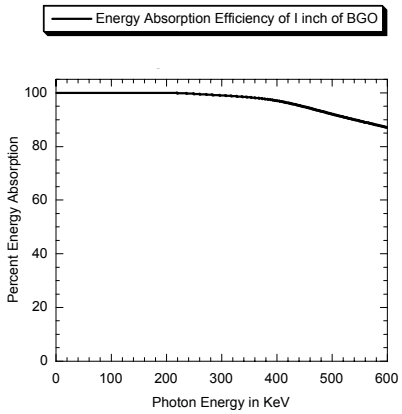

Figure 3. The energy absorption of photons traveling through 1 inch of BGO. This may be the physics behind the dip in detector energy response near 511KeV.

B. Current Simulation Accuracy

Summed profiles of a measured sinogram and a simulated sinogram using the new calculated energy response of a 3D PET scan and the corresponding simulation sinogram are in figure 4. A long emission scan, a long transmission scan, and the simple shape of the subject resulted in very accurate input images and corresponding simulation sinograms. There are predictable errors in some other profiles of this simulation due to energy response variability due to block effects and variability in the BGO penetration length.

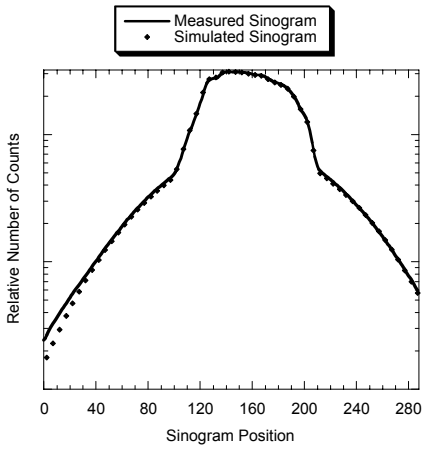

Figure 4. Summed sinogram profiles of simulated sinograms once detector energy response was adjusted.

It is important to simulate many different PET scans to make sure the accuracy is consistent for various activity distributions and attenuation maps. We simulated an adult thorax phantom using the simulated energy response calculated using a cylindrical phantom and compared resulted to measured sinogram data, see figure 5. The scatter tails of this graph match of fairly well. The error on the right side of this profile is due to structural errors in input images.

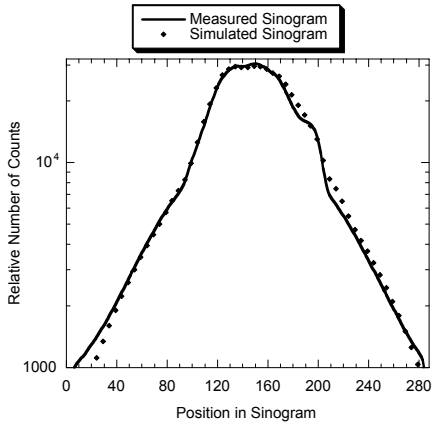

Figure 5. Summed sinogram profiles of simulation of thorax phantom compared to the summed measured sinogram profiles.

C. Fine Tuning Simulation Alignment

To improve the alignment of the simulation, a digital grid of point sources was simulated, and the resulting sinogram was reconstructed using the FBP algorithm on an ECAT HR+. By comparing the resulting image with the original grid, we could make sure the image volume was properly centered in the simulation, verify voxel size in all three directions, and properly align the angles and positions used to bin coincidence events in the simulated sinograms.

When the original grid was properly aligned with the reconstructed image, the transaxial voxel size was .52cm. This suggested that the nominal transaxial voxel size of .50625cm for the FBP reconstruction algorithm used on the scanner was incorrect. To verify results, a transmission scan was performed on a 52.4cm aluminum rod. The length of the

rod in the reconstructed transmission image was 101 voxels. This implies .519cm voxel size, confirming simulated results.

B Distribution of the 602keV Coincidence Events

Our initial simulation for ^{124}I only took into account positron emissions and positron emissions in coincidence with a 602KeV photon. This version was too slow to use for image correction, so we analyzed simulated distributions of coincidence events involving gamma rays and developed a fast analytical correction method in the following manner.

Through simulation, we obtained distributions of the detected events of an annihilation photon in coincidence with a 602Kev photon. To reduce noise, we summed all profiles from the first 72 angles and, separately, the last 72 angles of the simulated sinogram of the Jaszczak phantom. We found that both sinogram profile distributions had linear gradients, and the slope of these gradients depended on the sinogram profile's angle.

We also summed simulated profiles of the Jaszczak phantom from the bottom 31 planes and, separately, from the top 31 planes. These distributions also have a predictable linear gradient, and, although the scale of the distributions differed, the slope of the gradient was the same for different planes.

We saw these same effects in simulations of a thorax phantom. We expect that unless there is drastic change in the general location of the activity distribution across the 15cm gantry of the scanner that similar effects would be observed for most subjects. The flat nature of the distribution results from the random correlation of 511keV and 602keV photons and has little structure resulting from the geometry of the subject. This distribution differs greatly from sinogram distributions resulting from scatter events.

Because the gamma ray distribution is so predictable, we developed a simple correction for these events. By summing the normalized measured sinogram across planes to reduced noise, a good estimation of the slope of the linear distribution for the gammy ray coincidence events for various angular projections can be obtained. By scaling and subtracting these distributions from appropriate individual measured sinogram projections, an approximate data correction for these gamma ray events can be performed. Images reconstructed with and without using this correction are shown in figure 6.

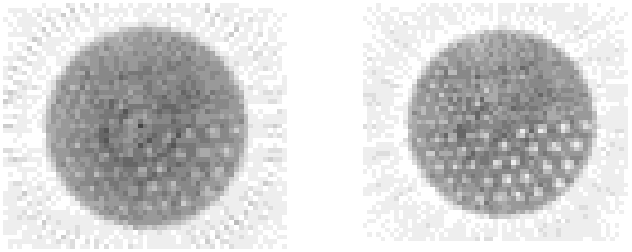

Figure 6. On the left is an image of a 3D PET scan of a Jaszczak phantom reconstructed without correction. On the right is the same scan reconstructed with the calculated data correction.

The improvement in contrast is observed in the corrected image; however, significant errors can occur using this correction. These errors can be aggravated especially when it is used in conjunction with a scatter correction that scales the calculated scatter distribution to measured scatter tails.

We found the ^{124}I activity significantly affected the accuracy of the transmission scan. Because only ~10% of ^{124}I decay are pure positron emissions, the relative singles rate would be effected by a factor of ~10 compared to a tracer such as FDG. This results in an artificial increase in detected coincidence events in the transmission scan and lowers measured attenuation values in the reconstructed transmission image volume. The extent of this effect is function of amount of activity in the scanner. For our scan of a Jaszczak phantom, we had to increase attenuation values by ~15% before accurate results were obtained.

This version is too slow to use as a Monte Carlo data correction for clinical image reconstruction. We have developed a new version that takes into all coincidence emissions and is faster than this version, but we must still use the quick analytical method to increase the accuracy of the activity map used in the new simulation.

C. New ^{124}I Simulation

Our current ^{124}I simulation incorporates over 99% of all possible coincidences that can result when I^{124} decays. This code is much more complex than the initial version and simulates 31 different possible coincidence emissions. The accelerated ^{124}I simulation currently simulates .8 million gamma events, 1 million scatter events, and .6 million primary events per minute. With this efficiency, the code is approaching clinical feasibility. To demonstrate the accuracy of this code we compared summed simulation sinogram profiles to normalized measured sinograms, see figure 7. We are working to fix the simulation artifact that can be seen at the ends of the sinogram. Some individual profiles (not shown) are less accurate due to the varying penetration length in BGO, block effects, and input image errors.

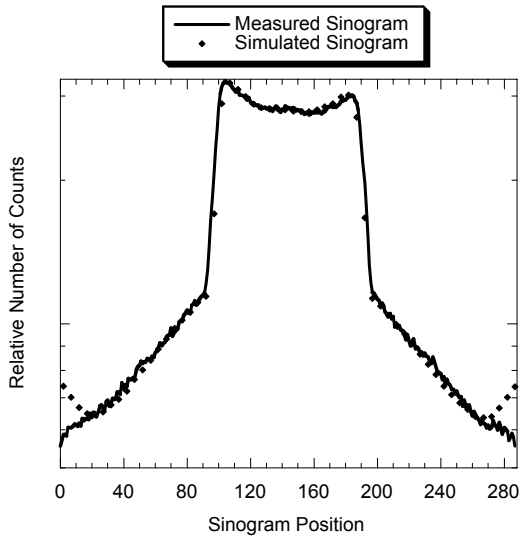

Figure 7. The simulated sinogram closely matches the measured sinogram for the total summed profile.

We separated gamma ray events, scatter events, and primary events of a simulated sinogram so the distinctive

shapes of the three different types could be observed. There is no similarity between the distribution of gamma coincidences and the distribution of scatter coincidences.

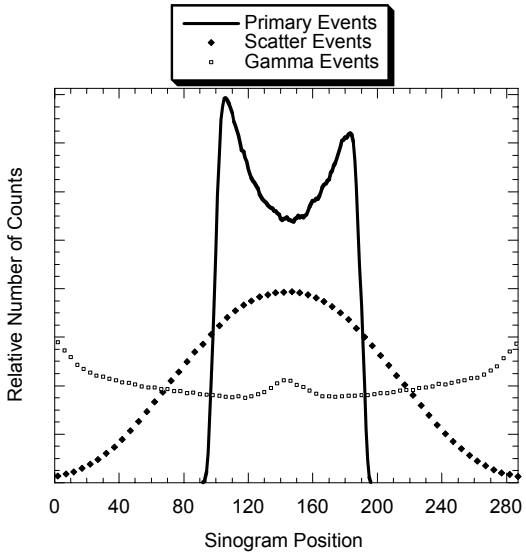

Figure 13. Simulated sinograms for three different types of distributions from the new simulation. The bumps at the ends and in the center of the gamma events graph are simulation artifacts.

IV Conclusion

The effectiveness of our simulation as an efficient research tool has been demonstrated. The detector energy response was evaluated, and we found that scattered photons with energies near 450keV have greater detection efficiency than higher energy annihilation photons. The energy absorption of 1 inch of BGO for 511keV photons corroborates this finding. Results also suggested that the voxel size of .50625cm assigned by the scanner's reconstruction code was incorrect. Actual voxel size was observed to be .52 ± .05cm.

The new Monte Simulation designed for 3D PET scans using I^{124} has the potential to become a fast, highly accurate, and clinically feasible image correction. We want to improve the accuracy of our original simulation by incorporating block effects and crystal penetration lengths into the model. We plan to continue improving the efficiency of the ^{124}I simulation. We are also currently developing a microPET simulation for PET scans using ^{124}I. We want to construct a website and make all simulation codes publicly available and easily accessible as soon as possible.

V. Acknowledgments

The authors would like to thank Dr. Charles Watson for valuable discussions. We would also like to thank David McElroy, Larry Pang, and Ron Sumida for assistance with phantom scans. This work was funded in part by NCI grant R01-CA56655 and DoE Contract DEF G0387-ER6061.

VI. References

[1] C.C. Watson, "A technique for measuring the energy response of a PET tomograph using a compact scattering source," *IEEE Transactions on Nuclear Science*, vol. 44, pp. 2500–2508, December 1997.

[2] K. S. Pentlow, M. C. Graham, R. M. Lambrecht, N. K. Cheung, and S. M. Larson, "Quantitative imaging of I-124 using positron emission tomography with applications to radioimmunodiagnosis and radioimmunotherapy," *Medical Physics*, vol. 18, pp. 357-66, 1991.

[3] C.H. Holdsworth, C.S. Levin, M. Janecek, M. Dahlbom, and E. J. Hoffman, "Performance analysis of an improved Monte Carlo simulation and scatter correction for 3D PET," *IEEE Transactions on Nuclear Science,* accept for publication December 2001.

[4] C.H. Holdsworth, C. S. Levin, M. Janecek, M. Dahlbom, and E. J. Hoffman, "Investigation of accelerated Monte Carlo techniques of PET simulation and 3D PET scatter correction," *IEEE Transactions on Nuclear Science*, vol. 48, pp. 74-81, February 2001.

[5] C.C. Watson et al, "Evaluation of simulation-based scatter correction of 3D Cardiac Imaging," *IEEE Transactions on Nuclear Science*, vol. 44, pp. 90-97, February 1997.

[6] I. Castiglioni, O. Cremonesi, M.C. Gilardi, V. Bettinardi, G. Rizzo, A. Savi, E. Bellotti, and F. Fazio, "Scatter correction techniques in 3D PET: a Monte Carlo evaluation," *IEEE Transactions on Nuclear Science*, vol.46, pp. 2053-2058, December 1999.

[7] C.J. Thompson, J.M. Cantu, and Y. Piccard, "PETSIM: Monte Carlo program simulation of all sensitivity and resolution parameters of cylindrical positron imaging systems," *Physics in Medicine and Biology*, vol. 37, pp. 731-749, 1992.

[8] D.R. Haynor, R.L.Harrison, et. al, "Improving the efficiency of emission tomography simulations using variance reduction techniques," *IEEE Transactions on Nuclear Science*, vol. 37, pp. 749-753, April 1990.

[9] H. Zaidi, A Scheurer, and C. Moral, "An object-oriented Monte Carlo simulator for 3D positron tomographs," Computer Methods and Programs Biomedcine, vol. 58, pp. 133-145, 1999.

[10] I. Castiglioni, INB-CNR, Milana University, H S. Raffaele Institute, Milano, Italy, personal communication, June 2000.

[11] H. Zaidi, "Relevance of accurate Monte Carlo modeling in nuclear medical imaging," *Medical Physics*, vol. 26, pp. 574-608, April 1999.

Send Correspondence To:
Clay Holdsworth
choldsworth@mednet.ucla.edu